RSC Advances

PAPER

View Article Online
View Journal | View Issue

Cite this: *RSC Adv.*, 2022, **12**, 22082

Production of *Cardamine violifolia* selenium-enriched peptide using immobilized Alcalase on Fe_3O_4 modified by tannic acid and polyethyleneimine

Shiyu Zhu, †[ab] Xin Cong,†[c] Zheng Sun,[d] Zhe Chen,[d] Xu Chen,*[ab] Zhenzhou Zhu, *[ab] Shuyi Li [ab] and Shuiyuan Cheng[ab]

Enzymatic synthesis of selenium (Se)-enriched peptides is vital for their application in supplementing organic Se. However, the poor stability and reusability of the free enzyme impedes the reaction. In this work, a highly stable immobilized Alcalase was synthesized by immobilizing Alcalase on tannic acid (TA) and polyethyleneimine (PEI) modified Fe_3O_4 nanoparticles (NPs). The optimal immobilization conditions for immobilized Alcalase were found at a TA/PEI (v/v) ratio of 1 : 1, pH of 10, and temperature of 40 °C, and the results from scanning electron microscopy (SEM), transmission electron microscopy (TEM), Fourier Transform Infrared (FTIR) and X-ray photoelectron spectroscopy (XPS) characterization confirmed the successful immobilization of Alcalase. The results of an enzyme property test showed that immobilized Alcalase had higher thermal and pH stability than free Alcalase, and retained 61.0% of the initial enzyme activity after 10 repetitions. Furthermore, the organic Se content of Se-enriched peptide prepared through enzymatic hydrolysis of *Cardamine violifolia* (CV) protein with immobilized Alcalase was 2914 mg kg^{-1}, and the molecular weight was mainly concentrated in 924.4 Da with complete amino acid components. Therefore, this study proposes the feasibility of immobilized enzymes for the production of Se-enriched peptides.

Received 19th June 2022
Accepted 25th July 2022

DOI: 10.1039/d2ra03765c

rsc.li/rsc-advances

1 Introduction

As a necessary micronutrient for human health, Se has the effects of delaying aging, enhancing immune function, and preventing cancer.[1–3] A deficiency in Se intake apparently affects the function and metabolism of gut microbes and even causes certain diseases such as Keshan disease.[4] Therefore, Se supplements in daily life have become a hotspot in nutrition research. However, Se can't be synthesized by the body itself, but must be obtained from various foods in the diet, which depend mainly on the concentration of Se in the soil. Previous studies have confirmed that organic Se is more available to the body compared to inorganic forms due to its higher safety and bioavailability.[5] Therefore, supplementing organic Se in the diet has attracted increasing attention over the past years.

Numerous studies have underlined that plant-based bioactive molecules are excellent ingredients that can be added to food to increase its nutrition.[6,7] In addition, they are generally suitable to act as natural carriers of organic Se.[7,8] In particular, Se-enriched peptide derived from Se-enriched plant are one of the most promising supplements for organic Se. The combination of Se and peptide not only enables Se to be more quickly absorbed in the body,[9] but also shows stronger bioactivity than original peptide.[10] The production of highly bioactive Se-enriched peptide by enzymatic hydrolysis of Se-enriched protein has received increasing attention recently. For example, Liu *et al.* purified Se-enriched antioxidative peptide from Se-enriched protein hydrolysates, and further studies revealed that the Se-enriched peptide exhibited strong antioxidative activity on DPPH$^{\bullet}$, OH^{-} and O_2^{-}, indicating the potential application of Se-enriched peptide as natural food antioxidant.[11] Zhang *et al.* prepared and identified Se-enriched peptide (M_w < 1 kDa) from Se-enriched soybeans, which could significantly mitigate organic oxidative damage in response to inflammation and senescence *via* MAPK/NF-κB pathway.[12] Tran *et al.* showed that pathogenic bacteria are able to be bound by covalent Se-labeled peptide and viruses, which are then killed

[a]*National R&D Center for Se-rich Agricultural Products Processing, Wuhan Polytechnic University, Wuhan, 430023, China. E-mail: zhushiyuu@126.com; chxu@whpu.edu.cn; zhenzhouzhu@126.com; lishuyisz@sina.com; s-y-cheng@sina.com*

[b]*School of Modern Industry for Selenium Science and Engineering, Wuhan Polytechnic University, Wuhan 430205, PR China*

[c]*Enshi Se-Run Material Engineering Technology Co., Ltd, Enshi 445000, Hubei, China. E-mail: 13905189777@163.com*

[d]*College of Food Science and Engineering, Wuhan Polytechnic University, Wuhan 430023, China. E-mail: sunzheng2013@outlook.com; zhechenkwy@163.com*

† These authors contributed equally to this work.

because of superoxide production.[13] Unlike these traditional Se-enriched plants, whose organic Se is mainly SeMet, the Se in CV is mainly SeCys. Our previous study found that Se polypeptide derived from the CV is rich in dipeptides and tripeptides and also has good antioxidant activity,[14] which can further fill the gap in the market of Se supplementation methods.

In spite of these advantages of Se-enriched peptide, the typical method of producing Se-enriched peptide, *i.e.*, enzymatic hydrolysis of Se-enriched proteins, still face some problems such as the poor reusability and inferior stability of free enzymes. The limits caused by free enzyme can be compensated by immobilizing the enzyme on a proper carrier, which can be separated from the system after the hydrolysis process is completed. Previous studies have reported the application of immobilized enzymes for the production of peptide through hydrolysis of soy protein,[15] rapeseed protein,[16] flaxseed protein,[17] sunflower protein,[18] and corn protein,[19] *et al.* However, studies on the production of Se-enriched peptides *via* hydrolysis with immobilized enzyme were relatively limited, such that further research on immobilized enzyme assisted hydrolysis of Se-enriched proteins is strongly required.

The goal of this study was to identify the feasibility of producing Se-enriched peptides *via* hydrolysis of CV with Alcalase immobilized on tannic acid and polyethyleneimine modified Fe_3O_4 NPs. Fe_3O_4 NPs were selected as carrier owing to the small size, magnetic, and ease of surface modification,[20] while TA and PEI modification were used to increase the biocompatibility of carrier and inhibit the agglomeration and oxidation of Fe_3O_4 NPs, which will facilitate the improvement the immobilized enzyme activity.[21,22] On the other hand, the preparation process of immobilized Alcalase, the structure of generated immobilized Alcalase, and their performance in enzymatic hydrolysis of CV was identified in detail to find a better method for efficient and stable recovery of Se-enriched peptide from CV. This study will aid in an improved understanding of efficient and stable production of Se-enrich peptide.

2 Experimental section

2.1 Materials

Fe_3O_4 dispersion (100–300 nm), tannic acid (TA), polyethyleneimine (PEI), methanol (CH_3OH) was purchased from Aladdin (Shanghai, China). Alcalase (2×10^6 U g^{-1}) from *Bacillus licheniformis* and casein (Tyr, 96%) were provided by Solarbio Co., Ltd (Beijing, China). Anhydrous ethanol (99.5%), boric acid (H_3BO_3), hydrochloric acid (HCl), trichloroacetic acid (TCA, 10%), potassium chloride (KCl), phosphoric acid (K_2HPO_4), sodium hydroxide (NaOH) and hydrochloric acid (HCl) were supplied by Sinopharm Chemical Reagent Co., Ltd (Shanghai, China). Tris(hydroxymethyl) aminomethane (Tirs) was obtained from Biofroxx (Germany). All these reagents unless specially mentioned are of analytical purity.

CV was obtained from Enshi.[14] The feedstock was milled and sieved to produce a granular powder with a particle size <150 μm before experiments.

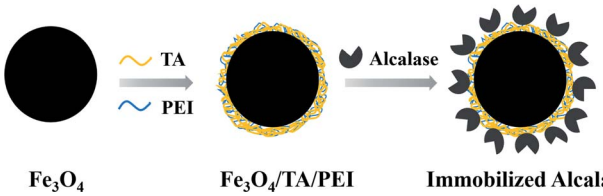

Fig. 1 Process of immobilization Alcalase.

2.2 Preparation of Fe_3O_4/TA/PEI carrier

The coating of TA and PEI on Fe_3O_4 was formed by the method of Wu *et al.* with slight modifications.[23] Firstly, 2 g of PEI was solubilized in 200 mL Tris–HCl buffer solution (10 mM, pH = 8.5) to produce 10 g L^{-1} PEI solution, and 2 g of TA was soluble in the same buffer solution to fabricate 2 g L^{-1} TA solution. Then, TA solution and PEI solution were mixed in a volume ratio of 5 : 1 to configure 20 mL of TA/PEI solution. Next, Fe_3O_4 NPs was treated with anhydrous ethanol combining ultrasonic treatment and then washed with deionized water to make it disperse uniformly. Finally, 100 mg treated Fe_3O_4 NPs was mixed into the mixed TA/PEI solution and then stirred at 150 rpm for 1 h at 25 °C, and washed with deionized water to obtain a stable Fe_3O_4/TA/PEI carrier.

2.3 Preparation of immobilized Alcalase

8 mg of Alcalase was firstly dissolved into 20 mL H_3BO_3 buffer solution (pH = 10), and then the above-mentioned Fe_3O_4/TA/PEI carrier was added in the solution and stirred at 45 °C with 150 rpm for 2 h (seeing in Fig. 1). After that, immobilized Alcalase was isolated from the solution by applied magnetic field and cleaned by deionized water until no residual free Alcalase was detected in the cleaning fluids. Finally, immobilized Alcalase was stored in anhydrous ethanol at 4 °C for further use.

2.4 Optimization of the immobilization process

In this section, the influence of TA/PEI volume ratio, temperature, and pH on immobilization process were studied. In detail, the TA/PEI (V/V) was adjusted to 5 : 1, 2 : 1, 1 : 1, 1 : 2, and 1 : 5, at immobilization temperature of 45 °C and pH = 10 to identify the influence of TA/PEI volume ratio on immobilization process. The pH was adjusted to 8, 9, 10, 11, and 12, at TA/PEI (V/V) of 1 : 1 and immobilization temperature of 45 °C to identify the effect of pH during immobilizing. The immobilization temperature was realigned to 35 °C, 40 °C, 45 °C, 50 °C, and 55 °C, at TA/PEI (V/V) of 1 : 1 and pH = 10 to identify the influence of immobilization temperature on immobilization process. The enzyme loading and enzyme activity recovery rate of immobilized Alcalase were chosen as key evaluation indicators to determine the optimal immobilization conditions.

The enzyme loading was determined by BCA protein concentration kit using the following equation:

$$\text{Enzyme loading rate } (\%) = \frac{C_0 - C_R - C_W}{C_0} \times 100\% \quad (1)$$

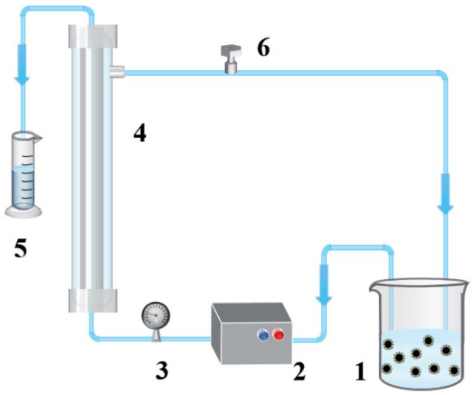

Fig. 2 The process of enzymatic hydrolysis of CV protein (no. 1 = reaction tank, 2 = peristaltic pump, 3 = pressure gauge, 4 = ultrafiltration membrane, 5 = retentate liquid valve, 6 = circulating valve).

where C_0, C_R, and C_w are the protein concentrations (mg mL^{-1}) in the original solution, the remaining solution, and cleaning fluids, respectively.

The enzyme activity recovery rate was defined as the ratio of immobilized Alcalase activity to Alcalase activity, and it was calculated by the following equation:

$$\text{Enzyme activity recovery rate } (\%) = \frac{U_1}{U_2} \times 100\% \quad (2)$$

where U_1 and U_2 are enzyme activity (U) of immobilized Alcalase and Alcalase, respectively. The enzyme activity (U) of immobilized Alcalase and Alcalase was tested with the following process. Casein solution (20 mL, 0.2 mM) was mixed with immobilized Alcalase or Alcalase under the same amount of Alcalase in H_3BO_3 buffer solution (pH = 10) and stirred at 40 °C for 30 min, after which the undigested casein was precipitated by adding excessive TCA (10%) to stop the hydrolysis reaction. After the reaction, the mixture was cooled to 25 °C and its absorbance was measured at 280 nm. An enzyme activity unit (U) was defined as the amount of tyrosine released at 1 μg per minute.

2.5 Enzymatic properties assay of Alcalase and immobilized Alcalase

2.5.1 Effect of hydrolysis pH and temperature on enzyme activity. The effects of hydrolysis pH (9–13) and temperature (30–70 °C) on enzyme activity of Alcalase and immobilized Alcalase were further performed, and the test procedure for enzyme activity can be seen in Section 2.4. The optimal hydrolysis condition is determined by the relative activity, which is defined as the ratio of the activity at a certain condition to the highest value in the same group, and is obtained by the following equation:

$$\text{Relative activity } (\%) = \frac{A_i}{A_{max}} \times 100\% \quad (3)$$

where A_i is the enzyme activity under a certain condition and A_{max} is the highest enzyme activity under a specific condition.

2.5.2 Storage stability and reusability. To evaluate the storage stability of free and immobilized Alcalase, the enzyme was kept in deionized water at 4 °C and its activity was tested at the optimal condition every 5 days for up to 30 days. As to the reusability of immobilized Alcalase, the consumed immobilized Alcalase was separated out with an applied magnetic field and washed several times at the end of each hydrolysis process. Then, the collected immobilized Alcalase was used in repeated hydrolysis procedure with the same condition. The reusability of the immobilized Alcalase was ascertained by the ratio of enzyme activity per cycle to initial activity, which was regarded as 100%.

2.6 Characterization

SEM (Quanta 450FEG, FEI, America) was used to determine the particle size and morphology at an acceleration voltage of 3.0 kV and resolution of 1.4 nm@1 kV. TEM (Teenai G2 F30 S-Twin, FEI, America) imaging was performed with an electron gun (LaB_6), at an acceleration voltage of 200 kV, point resolution of 0.248 nm, and line resolution of 0.144 nm. FTIR (Nexus 670, ThermoFisher Scientific, China) spectra was used to determine the main constituents present in the particles at a wavenumber range of 4000–400 cm^{-1}. We present the survey spectrum (binding energy range of 0–1350 eV) measured at a scanning width of 1 eV by XPS (ESCALAB 250Xi, ThermoFisher Scientific, China) to identify the chemical composition of immobilized Alcalase. The X-ray source is a monochromated Al Ka Alpha line.

2.7 Se-enriched peptide preparation from CV by immobilized Alcalase assisted hydrolysis

2.7.1 Extraction of CV proteins. CV protein was extracted by alkali-solution and acid-isolation method.[24] The powder of CV was dissolved in NaOH solution (100 mM) at a solid/liquid ratio of 1 : 40 (g mL^{-1}), followed by incubation at 50 °C for 8 h. The

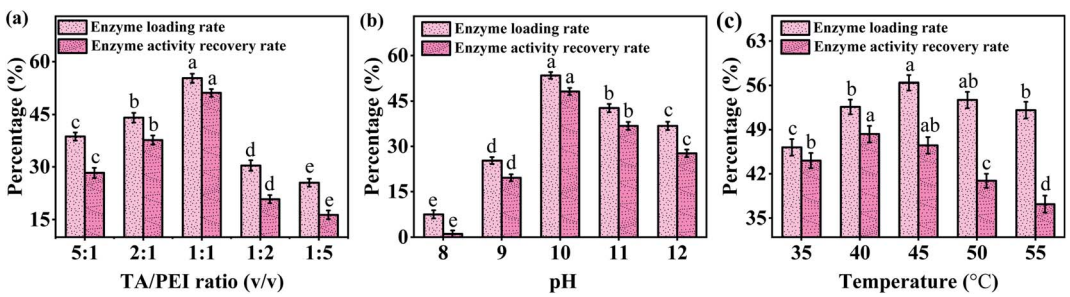

Fig. 3 The enzyme loading and activity recovery rate under different (a) TA/PEI ratio, (b) pH, and (c) temperature.

extracts were then concentrated 4 times with a rotary evaporator and left overnight at 4 °C after the pH was regulated to 3.5, after which the precipitate was collected by centrifugation at 4000 rpm for 15 min and lyophilized to obtain CV protein powder.

2.7.2 Enzymatic hydrolysis of CV proteins. The prepared CV protein was dissolved in deionized water to obtain protein solution with a substrate concentration of 2% (m/v). 3 L above protein solution was added to the enzymatic reactor, and the pH was adjusted to 11 by adding moderate NaOH solution (2 mol L^{-1}). Next, a certain amount (250–650 mg) of immobilized Alcalase was added to the protein solution, and the enzymatic reaction was kept at 50 °C for 1.5 h. Then, the peristaltic pump was turned on and worked at a pressure of 0.2 MPa for 1 h, such that the enzyme hydrolysis solution passed through the ultrafiltration membrane. The retentate liquid was returned to the reactor to continue the enzymatic hydrolysis process, and the permeate liquid was received for subsequent experiments (seeing in Fig. 2). To maintain the equilibrium of the reaction system, NaOH solution (2 mol L^{-1}) was added continually during this process. After the hydrolysis process was finished, the ultrafiltration membrane separation device was cleaned. The DH (degree of hydrolysis) of CV proteins was calculated by the pH-stat method, the details can be seen in previous study.[14]

2.8 Measurement of Se content and amino acid fraction of Se-enriched peptide

Total Se content was tested by atomic fluorescence spectrometry according to our previous study,[14] and the inorganic Se amount was determined by HPLC-AFS method with the following detailed conditions: negative high voltage of 240 V, Se lamp current of 45 mA, atomization temperature of 200 °C, carrier gas flow rate of 300 mL min^{-1}, shielding gas flow rate of 800 mL min^{-1}. The separation of Se species was realized using an anion exchange column (PRP-X100, 4.1 mm × 250 mm, 10 μm) at 25 °C with a flow rate of 1.0 mL min^{-1}, and the mobile phase is a homogeneous mixture of equal amounts of KH_2PO_4 (40 mM) and KCl (20 mM) using isocratic elution.

The organic Se content is calculated by total Se minus inorganic Se. GB 5009.124–2016 "Determination of amino acids in food" (Chinese national standard) was used to determine the amino acid by automatic amino acid analyzer (L-8900), and the details can be seen our previous study.[14]

2.9 Statistical analysis

All our experiments were repeated three times and the data was analyzed by using SPSS 19.0. Deference between individual experiments were treated using analysis of variance (ANOVA)

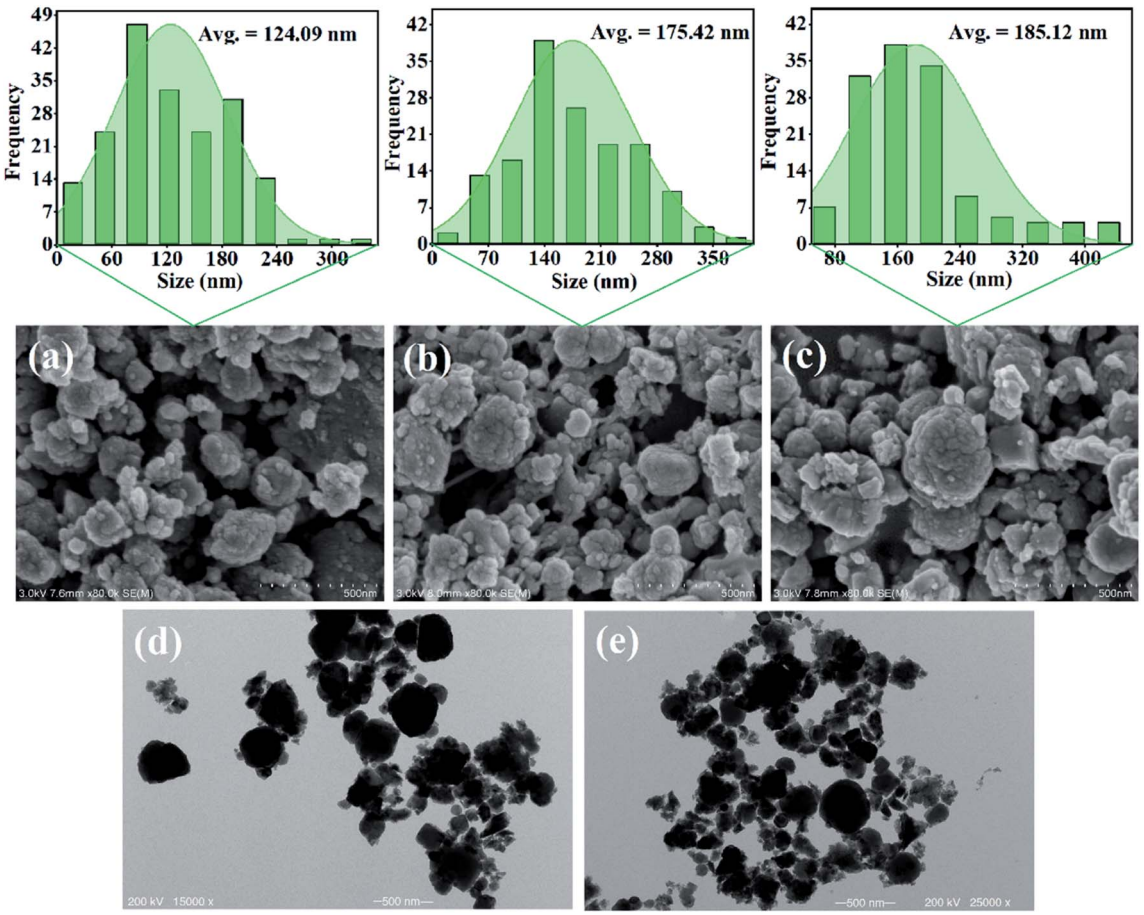

Fig. 4 SEM images of the magnetic (a) Fe_3O_4 NPs, (b) Fe_3O_4/TA/PEI carrier, and (c) immobilized Alcalase. TEM images of magnetic (d) Fe_3O_4 NPs and (e) immobilized Alcalase.

and compared by Ducan's range test to a significance level of 5%. All results are expressed as mean ± standard deviations.

3 Results and discussion

3.1 Alcalase immobilization

3.1.1 Single-factor experiment of Alcalase immobilization. Alcalase was immobilized on Fe_3O_4 through the bridge of TA coating, and the mechanical stability of the coating is improved by the addition of PEI due to its cross-linking effect.[25] Hence, it was speculated that the ratio of TA to PEI will influence the enzyme loading and activity recovery rate. As can be seen in Fig. 3a, the enzyme loading and activity recovery rate increased rapidly with TA/PET ratio decreasing before it was up to 1 : 1, and then decreased with TA/PET ratio decreasing further. The results were similar to the findings reported by Ran *et al.*,[26] and the possible reason for the decreased enzyme loading and activity recovery rate of Alcalase at lower TA/PEI ratio may be that the available adsorption sites on TA coating become saturated, and excess PEI inhibits the interaction between TA coating and Alcalase.[26]

As seen in Fig. 3b, the enzyme loading and activity were peaked at pH of 10. The reason is that, under strong bases conditions (pH 11 and 12), the biological activity of enzymes as proteins is destroyed, since their spatial structure and secondary bonds was disrupted. On the other hand, under weak alkaline conditions (near pH 8.5), the pyrogallol groups in TA oligomers is readily oxidized to quinone groups and further cross-linked with the amine group of PEI due to Schiff base/Michael addition reaction,[27] and thus little active sides of TA coating was left to immobilize Alcalase. In addition, the temperature–activity curve of the enzyme (Fig. 3c) showed that the enzyme activity increased with increasing temperature, when the enzyme distribution on Fe_3O_4/TA/PEI carrier was accelerated, so that the adsorption rate was the main limiting factor of the enzyme activity. With further increase in temperature, the enzyme activity decreases sharply, at which time the thermal stability shift of the enzyme conformation turns to be the main constraint.[28] Overall, considering the enzyme loading and activity, a TA/PEI ratio of 1 : 1, pH of 10, and temperature of 40 °C were chosen to carry out the subsequent experiments.

3.1.2 Properties of immobilized Alcalase. The Alcalase was immobilized under the optimal conditions mentioned above, and scanning electron microscopy analysis was performed to compare its surface morphologies with Fe_3O_4 NPs and magnetic Fe_3O_4/TA/PEI carriers. As shown in Fig. 4a, Fe_3O_4 NPs have approximately spherical structure and good dispersion (average diameter of 124 nm). After modifying with TA and PEI, the spherical structure of carrier was kept and no obvious agglomeration phenomena was found, contributing to the efficiency of the immobilized enzyme.[29] Meanwhile, the average diameter of the NPs increased to 175 nm, which can be attributed to formation of TA/PEI coating. Similarly, the particle size of Fe_3O_4/TA/PEI after immobilization of Alcalase was further increased to 185 nm owing to the integration of enzymes with NPs.[30] The TEM morphology of immobilized Alcalase show a core–shell structure (Fig. 4e), and the central black area was Fe_3O_4 NPs, surrounded by a very thin gray layer visible, which should be a uniformly dispersed coating formed by TA and PEI cross-linking.[31]

To confirm the successful adhesion of TA–PET coating and the effective immobilization of Alcalase, the FTIR spectra of Fe_3O_4 NPs, Fe_3O_4/TA/PEI carrier and immobilized Alcalase by analyzed. As shown in Fig. 5a, two new peaks at 1342 cm^{-1} and 1534 cm^{-1} were observed after the modification of Fe_3O_4 carrier by TA and PEI. The new peaks at 1342 cm^{-1} and 1534 cm^{-1} were assignable to phenol groups and N–H stretching vibration,[29,32] respectively, suggesting the successful loading of TA and PEI on Fe_3O_4 NPs. Meanwhile, the peak at 1639 cm^{-1} was the characteristic absorption peak of C=N, which confirmed the Schiff base reaction between TA and PEI.[29,30,32] Furthermore, XPS analysis was conducted to verify the successful preparation of AP@ Fe_3O_4/TA/PEI. As shown in Fig. 5b, the stronger peak at 285.25 eV and 400.09 eV is the characteristic peak of C element and N element, respectively, suggesting that Alcalase was successfully immobilized on TA/PEI coated Fe_3O_4 NPs.

3.1.3 Performance evaluation of immobilized Alcalase. The temperature response on the relative activity of the free and

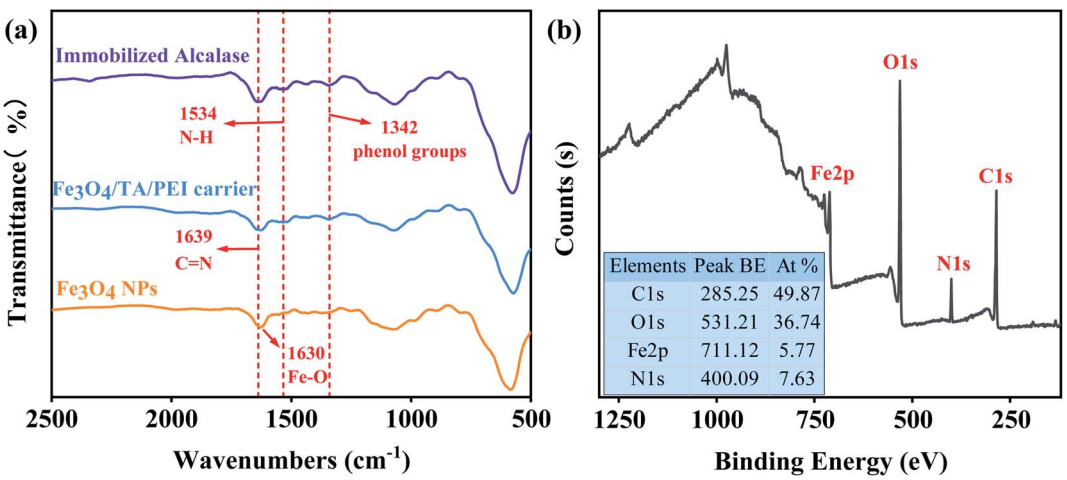

Fig. 5 FTIR of (a) magnetic Fe_3O_4 NPs, Fe_3O_4/TA/PEI carrier and immobilized Alcalase. XPS survey spectra of (b) immobilized Alcalase.

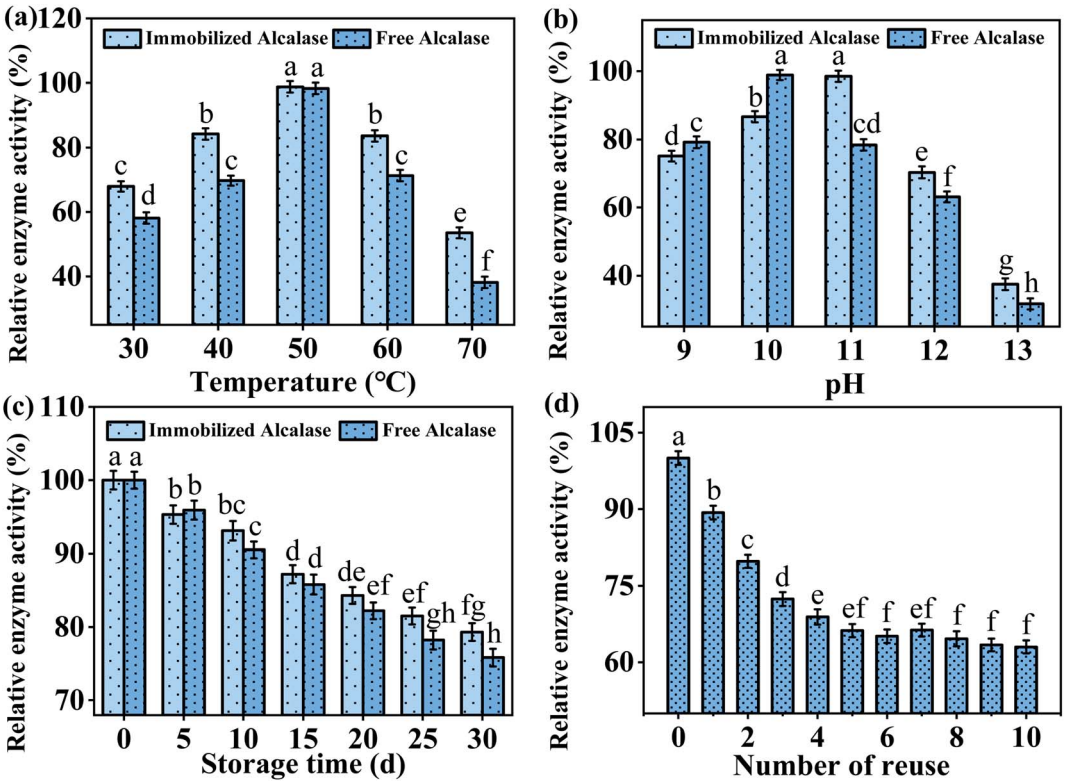

Fig. 6 Effect of (a) temperature, (b) pH, (c) storage time on relative enzyme activity, and (d) number of reuses.

immobilized Alcalase is showed in Fig. 6a. The optimal temperature for both immobilized Alcalase and free Alcalase were 50 °C, yet immobilized Alcalase was less affected by temperature than free Alcalase and maintained high enzyme activity over a wider temperature range. This may be owing to the multi-stage mesh structure of TA/PEI coating, providing some protection to the Alcalase, thus improving the temperature resistance and inhibiting the destroy of spatial conformation of enzyme at high temperatures.[33,34]

The effect of pH (9–13) on the activity of free and immobilized Alcalase was also investigated, and the results are compared in Fig. 6b. The optimum pH of free Alcalase is 10, while the optimum pH of immobilized Alcalase rises to 11 with improved pH tolerance compared to free Alcalase. The result was similar to previous studies wherein the optimal pH of the enzyme increased after immobilization, which may be explained by the fact that the immobilization process changed the net charge distribution of enzyme.[19,35,36]

Further, the storage stability of immobilized Alcalase and Alcalase were tested by storing these enzymes at 4 °C for 30 days, during which the relative enzyme activity was identified every 5 days. After one month of storage, the immobilized Alcalase maintained 79.3 ± 1.2% enzyme activity, obviously higher than that of free Alcalase (75.8 ± 1.2%). The autosolubility of free Alcalase may lead to a severe decrease in its relative activity, while the interaction between Alcalase and Fe_3O_4/TA/PEI may contribute to a higher conformational stability of Alcalase.[37,38]

It is known that the most outstanding advantage of enzyme immobilization is that the enzyme can be easily separated from the reaction system and reused for several times. To explore the potential of immobilized Alcalase for industrial applications, its reusability was further investigated. As shown in Fig. 6d, an obvious decrease in the enzyme activity of immobilized Alcalase was found at the first four cycles. This may be attributed to that part of Alcalase was not connected with the Fe_3O_4/TA/PEI carrier firmly, leading to enzyme leakage during the recycling process.[39] After the first four cycles, the activity of immobilized Alcalase reduced gently, probably because of the slow inactivation of

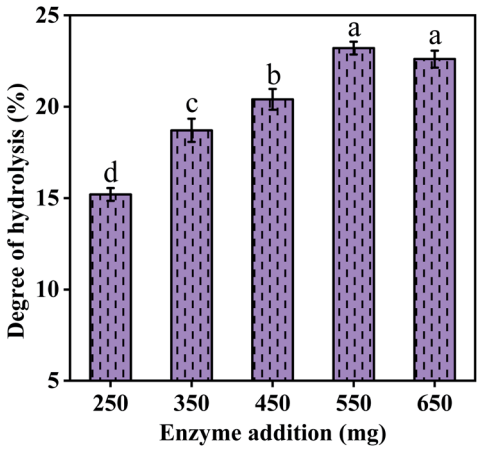

Fig. 7 Hydrolysis of CV protein at different enzyme addition.

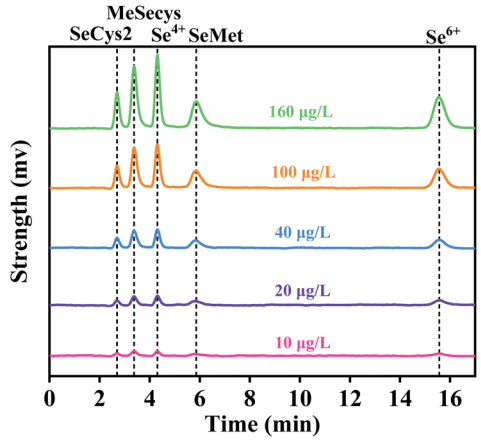

Fig. 8 Chromatogram of different forms of Se standard solutions.

Alcalase upon use.[40] Nevertheless, unlike the free Alcalase which could only be used once, the enzyme activity of immobilized Alcalase could still reach 61 ± 1.2% of the initial activity after 10 times reuse, which greatly reduced the costs.

3.2 Se-enriched peptide preparation

The prepared immobilized Alcalase were further used for the hydrolysis of CV protein to evaluate its application on the production of Se-enriched peptide, and the influence of enzyme addition amount on the DH of CV protein was identified. The temperature and pH were fixed at 50 °C and 11 to improve the activity of immobilized Alcalase according to the previous results (shown in Fig. 6). It can be seen from Fig. 7 that, the DH gradually increased with the increase of immobilized Alcalase addition, and reached the maximum when the immobilized Alcalase addition was between 550 mg and 650 mg, which was due to the fact that the increase of enzyme addition would directly promote the efficiency of enzyme hydrolysis. The optimum immobilized Alcalase addition was determined to be 550 mg, taking into account the cost factor.

Since the total and organic Se content is an important factor for the application of obtained se-enriched peptide, AFS and HPLC-AFS were used in this study to determine the total Se and distribution of Se species, respectively. Fig. 8 shows the chromatographs of the five common Se forms, which indicates that inorganic Se was well separated from the organic Se, enabling the accurate quantification of inorganic Se content. Based on the above discussion, the total and organic Se content of CV protein and CV peptide were calculated and presented in Table 1. It can be found that CV peptide shows high organic Se content, which reached up to 2914 ± 14 mg kg^{-1}, accounting for 93.1% of the total Se. In this context, CV peptide derived from the CV protein with immobilized Alcalase is a promising Se supplement.

Table 2 Analysis of amino acid fraction of CV peptide[a]

Amino acid type	Relative content (%)
Aspartic acid (Asp)	2.99
Threonine* (Thr)	3.56
Serine (Ser)	5.57
Glutamic acid (Glu)	6.52
Proline (Pro)	1.42
Glycine (Gly)	10.52
Alanine* (Ala)	12.22
Cysteine (Cys)	1.26
Valine* (Val)	7.06
Methionine* (Met)	4.03
Isoleucine* (Iso)	3.15
Leucine* (Leu)	11.28
Tyrosine (Tyr)	8.06
Phenylalanine* (Phe)	9.73
Histidine (His)	2.65
Lysine* (Lys)	7.31
Arginine (Arg)	2.68

[a] Note: * represents essential amino acids.

On the other hand, the amino acid composition of obtained Se-enriched peptide was analyzed, with results shown in Table 2. It can be found that the amino acids in the Se-enriched peptide are complete, and the main amino acids are alanine, leucine and glycine, followed by phenylalanine and tyrosine. In particular, alanine has the highest content, accounting for 12% of the total amino acids. Nevertheless, cysteine accounts for a relatively low percentage, which may be undetectable as Se substituted S is combined with cysteine amino acids.[41] In addition, the molecular weights of the Se-enriched peptide were mainly distributed in 739.3 Da (8.0%), 942.4 Da (75.7%) and 1013.4 Da (16.3%), indicating that the products were thoroughly enzymatically digested and the molecular weights were uniformly distributed.

Table 3 compares the degree of hydrolysis of proteins from different raw materials, including CV. We found that the degree of hydrolysis while using the Alcalase on Fe_3O_4 modified by TA and PEI was higher compared to other immobilized Alcalase. Meanwhile, although the degree of hydrolysis is similar to the free Alcalase of Wu *et al.*,[14] it has the advantages of reusability and economic savings, which can better enable the commercial mass production of Se-enriched peptide.

Table 1 Total and organic Se content of CV protein and CV peptide

Name of the sample	Total Se (mg kg^{-1})	Inorganic Se (mg kg^{-1})	Organic Se (mg kg^{-1})	Percentage of organic Se (%)
CV protein	5330 ± 31	660 ± 8	4670 ± 23	87.6
CV peptide	3130 ± 19	216 ± 4	2914 ± 14	93.1

Table 3 Process in enzymatic hydrolysis of protein

Raw material	Type of enzyme	Degree of hydrolysis	Reutilization	Ref.
CV	Immobilized Alcalase	23.2%	Yes	This study
CV	Alkaline protease and neutral protease	Not explored	No	42
CV	Alkaline protease	21.4%	No	14
Chickpea	Immobilized Alcalase	10%	Yes	43
Isolated rapeseed protein	Immobilized Alcalase	18.40%	Yes	16
Se-enriched rice protein	Se-enriched rice protein Alcalase	22.59%	No	44

4 Conclusion

In summary, we prepare an immobilized enzyme by using Alcalase as active component and TA and PEI modified Fe_3O_4 NPs as carrier. SEM, TEM, FTIR, and XPS results showed the successful synthesis of immobilize enzyme. Subsequently, after immobilization of Alcalase on Fe_3O_4/TA/PEI under optimal conditions, the obtained immobilized enzyme showed higher thermal and pH stability compared with the free enzyme, and retained 61.0% of the initial enzyme activity after 10 cycles. Moreover, the prepared immobilized Alcalase was applied for the preparation of Se-enriched peptide using CV protein as raw material. The Se-enriched peptide obtained from the optimal process shows an organic Se content of 2914 mg kg^{-1}, a molecular weight of 942.4 Da (75.7%), and a complete amino acid fraction. Therefore, this study provides the fundamental basis to immobilize Alcalase on Fe_3O_4 modified by TA and PEI, and solved the problem of enzyme stability and activity in producing Se-enriched peptides.

Author contributions

Shiyu Zhu: data curation; formal analysis; writing – original draft; Xin Cong: writing – review & editing; funding acquisition. Zheng Sun: investigation. Zhe Chen: investigation. Xu Chen: writing – review & editing; investigation. Zhenzhou Zhu: funding acquisition, supervision. Shuyi Li: investigation. Shuiyuan Cheng: funding acquisition.

Conflicts of interest

The authors declare no conflict of interest.

Acknowledgements

The authors acknowledge the support of Outstanding young and middle-aged science and technology innovation team in Hubei Province (T2020012), Key Research and Development Program of Hubei Province (2020BBA043), Scientific and Technology Project of Enshi Tujia & Miao Autonomous Prefecture (XYJ2020000021) and Key Innovation Team in Enshi Tujia and Miao Autonomous Prefecture, 2020.

References

1 H. Estevez, E. Garcia-Calvo, J. Rivera-Torres, M. Vallet-Regí, B. González and J. L. Luque-Garcia, *Pharmaceutics*, 2021, **13**, 356.
2 M. Y. Lee, A. Leonardi, T. J. Begley and J. A. Melendez, *Redox Biol.*, 2020, **28**, 101375.
3 K. Spyridopoulou, G. Aindelis, A. Pappa and K. Chlichlia, *Cancers*, 2021, **13**, 5335.
4 Z. Zhang, H. Xiang, G. Sun, Y. Yang, C. Chen and T. Li, *Genes Environ.*, 2021, **43**, 56.
5 M. Obieziurska, A. J. Pacuła, A. Laskowska, A. Długosz-Pokorska, A. Janecka and J. Ścianowski, *Materials*, 2020, **13**, 661.
6 Z. Guo, Y. Huang, J. Huang, S. Li, Z. Zhu, Q. Deng and S. Cheng, *Food Chem.*, 2022, **385**, 132702.
7 S. Li, H. Xu, Y. Sui, X. Mei, J. Shi, S. Cai, T. Xiong, C. Carrillo, J. M. Castagnini and Z. Zhu, *Foods*, 2022, **11**, 1552.
8 C. Xu, L. Qiao, Y. Guo, L. Ma and Y. Cheng, *Carbohydr. Polym.*, 2018, **195**, 576–585.
9 J. Zhang, S. Gao, H. Li, M. Cao, W. Li and X. Liu, *Food Sci. Nutr.*, 2021, **9**, 6322–6334.
10 J. Zhu, M. Du, M. Wu, P. Yue, X. Yang, X. Wei and Y. Wang, *Eur. Food Res. Technol.*, 2020, **246**, 1483–1494.
11 K. Liu, Y. Zhao, F. Chen and Y. Fang, *Food Chem.*, 2015, **187**, 424–430.
12 X. Zhang, H. He, J. Xiang, B. Li, M. Zhao and T. Hou, *Food Chem.*, 2021, **358**, 129888.
13 P. Tran, J. Kopel, J. A. Fralick and T. W. Reid, *Antibiotics*, 2021, **10**, 611.
14 M. Wu, Z. Zhu, S. Li, J. Cai, X. Cong, T. Yu, W. Yang, J. He and S. Cheng, *Food Biosci.*, 2020, **38**, 100743.
15 H. Zhu, Y. Zhang, T. Yang, D. Zheng, X. Liu, J. Zhang and M. Zheng, *LWT*, 2022, **162**, 113505.
16 B. Wang, T. Meng, H. Ma, Y. Zhang, Y. Li, J. Jin and X. Ye, *Ultrason. Sonochem.*, 2016, **32**, 307–313.
17 C. Wei, K. Thakur, D. Liu, J. Zhang and Z. Wei, *Food Chem.*, 2018, **263**, 186–193.
18 T. Sewczyk, M. Hoog Antink, M. Maas, S. Kroll and S. Beutel, *AMB Express*, 2018, **8**, 18.
19 Y. Wang, H. Chen, J. Wang and L. Xing, *Process Biochem.*, 2014, **49**, 1682–1690.
20 J. Wan, L. Zhang, B. Yang, B. Jia, J. Yang and X. Su, *Chem. Eng. J.*, 2022, **427**, 131976.

21 S. Sunoqrot, A. Al-Hadid, A. Manasrah, R. Khnouf and L. H. Ibrahim, *RSC Adv.*, 2021, **11**, 39582–39592.
22 B. Lin, H. Tan, W. Liu, C. Gao and Q. Pan, *RSC Adv.*, 2020, **10**, 16168–16178.
23 L. Wu, Q. Lin, C. Liu and W. Chen, *Polymers*, 2019, **11**, 1975.
24 S. Zhu, C. Du, T. Yu, X. Cong, Y. Liu, S. Chen and Y. Li, *J. Food Sci.*, 2019, **84**, 3504–3511.
25 S. Zhang, Z. Jiang, X. Wang, C. Yang and J. Shi, *ACS Appl. Mater. Interfaces*, 2015, **7**, 19570–19578.
26 F. Ran, Y. Zou, Y. Xu, X. Liu and H. Zhang, *Chem. Eng. J.*, 2019, **375**, 121947.
27 Q. Wei, K. Achazi, H. Liebe, A. Schulz, P. L. M. Noeske, I. Grunwald and R. Haag, *Angew. Chem., Int. Ed.*, 2014, **53**, 11650–11655.
28 W. Zhuang, J. Huang, X. Liu, L. Ge, H. Niu, Z. Wang, J. Wu, P. Yang, Y. Chen and H. Ying, *Food Chem.*, 2019, **275**, 197–205.
29 Q. Xiao, C. Liu, H. Ni, Y. Zhu, Z. Jiang and A. Xiao, *Food Chem.*, 2019, **272**, 586–595.
30 S. Moradi, F. Khodaiyan and S. Hadi Razavi, *Int. J. Biol. Macromol.*, 2020, **154**, 1366–1374.
31 J. Zhao, R. Luque, W. Qi, J. Lai, W. Gao, M. R. H. S. Gilani and G. Xu, *J. Mater. Chem. A*, 2015, **3**, 519–524.
32 V. Venezia, F. Sannino, A. Costantini, B. Silvestri, S. Cimino and V. Califano, *Microporous Mesoporous Mater.*, 2020, **302**, 110203.
33 S. Chen, Y. Xie, T. Xiao, W. Zhao, J. Li and C. Zhao, *Chem. Eng. J.*, 2018, **337**, 122–132.
34 J. Song, H. Shen, Y. Yang, Z. Zhou, P. Su and Y. Yang, *J. Mater. Chem. B*, 2018, **6**, 5718–5728.
35 A. Pal and F. Khanum, *Process Biochem.*, 2011, **46**, 1315–1322.
36 M. Khan, Q. Husain and R. Bushra, *Int. J. Biol. Macromol.*, 2017, **105**, 693–701.
37 K. Atacan and M. Özacar, *Colloids Surf., B*, 2015, **128**, 227–236.
38 B. Zhang, P. Li, H. Zhang, L. Fan, H. Wang, X. Li, L. Tian, N. Ali, Z. Ali and Q. Zhang, *RSC Adv.*, 2016, **6**, 46702–46710.
39 N. Elias, R. A. Wahab, L. W. Jye, N. A. Mahat, S. Chandren and J. Jamalis, *Cellulose*, 2021, **28**, 5669–5691.
40 M. Temkov, A. Petrovski, E. Gjorgieva, E. Popovski, M. Lazarova, I. Boev, P. Paunovic, A. Grozdanov, A. Dimitrov and A. Baidak, *Eng. Life Sci.*, 2019, **19**, 617–630.
41 C. Gabel-Jensen, K. Lunøe, K. G. Madsen, J. Bendix, C. Cornett, S. Stürup, H. R. Hansen and B. Gammelgaard, *J. Anal. At. Spectrom.*, 2008, **23**, 727–732.
42 Y. Lin, Y. Li, X. Cong, Y. Xia, D. Huang, S. Chen and S. Zhu, *J. Food Sci.*, 2022, **87**, 3235–3247.
43 M. del Mar Yust, J. Pedroche, M. del Carmen Millán-Linares, J. M. Alcaide-Hidalgo and F. Millán, *Food Chem.*, 2010, **122**, 1212–1217.
44 Y. Fang, X. Pan, E. Zhao, Y. Shi, X. Shen, J. Wu, F. Pei, Q. Hu and W. Qiu, *Food Chem.*, 2018, **275**, 696–702.